

MSGNN: Multi-scale Spatio-temporal Graph Neural Network for Epidemic Forecasting

Mingjie Qiu¹, Zhiyi Tan¹ and Bing-kun Bao^{1*}

¹The College of Telecommunications and Information Engineering, Nanjing University of Posts and Telecommunications, Nanjing, Jiangsu, China.

*Corresponding author(s). E-mail(s): bingkunbao@njupt.edu.cn;
Contributing authors: 1021010625@njupt.edu.cn;
tzy@njupt.edu.cn;

Abstract

Infectious disease forecasting has been a key focus and proved to be crucial in controlling epidemic. A recent trend is to develop forecasting models based on graph neural networks (GNNs). However, existing GNN-based methods suffer from two key limitations: (1) Current models broaden receptive fields by scaling the depth of GNNs, which is insufficient to preserve the semantics of long-range connectivity between distant but epidemic related areas. (2) Previous approaches model epidemics within single spatial scale, while ignoring the multi-scale epidemic patterns derived from different scales.

To address these deficiencies, we devise the Multi-scale Spatio-temporal Graph Neural Network (MSGNN) based on an innovative multi-scale view. To be specific, in the proposed MSGNN model, we first devise a novel graph learning module, which directly captures long-range connectivity from trans-regional epidemic signals and integrates them into a multi-scale graph. Based on the learned multi-scale graph, we utilize a newly designed graph convolution module to exploit multi-scale epidemic patterns. This module allows us to facilitate multi-scale epidemic modeling by mining both scale-shared and scale-specific patterns. Experimental results on forecasting new cases of COVID-19 in United State demonstrate the superiority of our method over state-of-arts. Further analyses and visualization also show that MSGNN offers not only accurate, but also robust and interpretable forecasting result.

Keywords: Epidemic Forecasting, Graph Neural Networks, Multi-scale Modeling, Graph Structure Learning, Spatio-temporal Forecasting.

1 Introduction

The infectious diseases pose a serious hazard to global public health. For decades, epidemic modelers have been struggling in forecasting the spread of emerging infectious diseases, such as the Zika virus, the Ebola virus, and most recently, the COVID-19 virus. To put the virus in control, accurate forecasting of the epidemic is of great significance for both individuals and administrators.

Recently, graph neural networks (GNNs) based methods have emerged as a promising way of combating epidemics. The core idea of these approaches is modeling the epidemic signals between different areas to learn the underlying patterns in historical data. For example, Earlier works (Rodríguez et al, 2021; Kapoor et al, 2020; Gao et al, 2021) view geographic adjacency as the key factor of trans-area epidemic signals, then directly apply graph convolution on a static spatial graph. Some follow-on studies (Ye et al, 2021; Zheng et al, 2021; Panagopoulos et al, 2021; Deng et al, 2020) extend the spatial graphs to spatio-temporal graphs, where the trans-area signals are dynamically measured. Most recently, a technical trend is to incorporate more epidemic-related factors (e.g. the social network data) into trans-area epidemic signals. These factors enrich the existing spatio-temporal graph representations (Fritz et al, 2022; Wang et al, 2022; Xie et al, 2023). Benefiting from the learned epidemic evolution patterns, existing GNN-based methods achieve promising performance in epidemic forecasting task.

Despite their effectiveness, it is noticeable that most of the previous GNN-based methods model epidemics at single spatial scale. We suggest these single-scale based methods fall short in two respects: (1) **Failing to preserve long-range connectivity.** Existing works stack multiple convolution layers to aggregate information step by step, which dilutes the long-range connectivity between distant areas. As shown in the left side of Figure 1, in single scale view, the epidemic transmission path from city A to city B goes through five hops, which means the trans-area epidemic signal may mix up with noise from another four cities. More importantly, the receptive fields of existing GNN-based methods are significantly limited due to *oversmoothing* issues (Chen et al, 2020). These studies fail to preserve the semantics of long-range connectivity, i.e., the high-order relation between distant but epidemic related areas, leading to limited performance. (2) **Ignoring the multi-scale epidemic patterns.** Previous GNN-based works only exploit epidemic patterns within single spatial scale. However, an important fact has been ignored: the epidemic evolves simultaneously at different scales and reflects multiple epidemic evolution patterns. For example, the fine-grained epidemic evolution depicts local epidemic evolution pattern, while the coarse-grained evolution contains broader regional epidemic pattern. Such multi-scale patterns provide useful

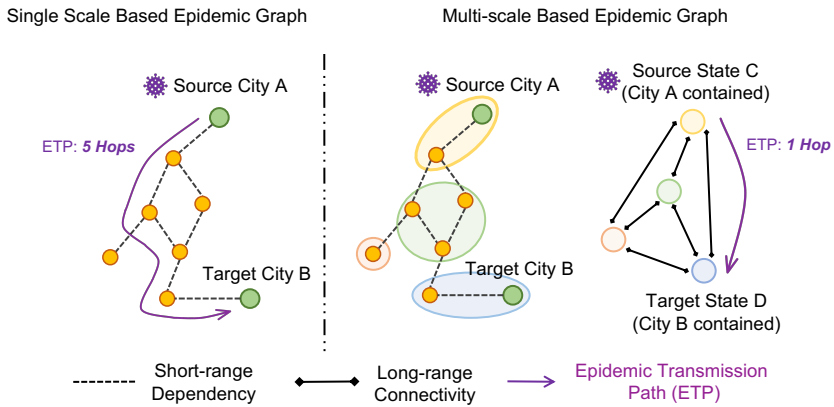


Fig. 1 A Comparison between single-scale based and multi-scale based epidemic spatio-temporal graph. The additional macro scale helps model long-range connectivity, which significantly reduces the hops of epidemic transmission path between distant areas.

information that can aid accurate epidemic forecasting. Therefore, it is important to extract epidemic patterns from different scales and conduct multi-scale modeling. Unfortunately, none of these works take these multi-scale epidemic patterns into consideration.

To this end, we propose the Multi-scale Spatio-temporal Graph Neural Network (MSGNN) for infectious disease forecasting. The model contains two components to solve the fore-mentioned challenges correspondingly: (1) **Graph Structure Learning Module.** Since the semantic of long-range connectivity is hard to preserve through single-scale modeling, in this module, we construct a multi-scale spatio-temporal graph to deal with different epidemic relations. As shown on the right side of Figure 1, the proposed multi-scale spatio-temporal graph contains two scales. In micro scales, we define the trans-area signal as short-range dependency, which is utilized to express fine-resolution spatial topology. Furthermore, considering the broader spatial effect of macro scale, we view trans-regional signals between states as long-range connectivity, which significantly reduce the epidemic transmission hops between distant areas. All signals are dynamically self-adjusted along with epidemic evolution, forming a multi-scale spatio-temporal graph as output. (2) **Multi-scale Graph Convolution Module.** Considering the discrepancy between different spatial scales, directly conducting inter-scale aggregation is not a viable option. Therefore, we devise a multi-scale information aggregation scheme to distill scale-specific and scale-shared parts from multi-scale patterns. This scheme first applies scale-specific message passing to obtain aggregated features at each scale. Then, the scheme distills the scale-shared epidemic patterns from multi-scale spatio-temporal graph. Finally, a multi-scale fusion block is introduced to integrate multi-scale features based on scale-shared patterns. These fused representations serve as the final output for forecasting.

To verify the effectiveness of proposed model, we choose the latest and one of the most prevalent infectious disease, the COVID-19 virus as the validation epidemic. We conduct a comprehensive result evaluation on the COVID-19 dataset of the US, which contains two administrative levels, i.e. county level for micro scale and state level for macro scale. The result shows that our model outperforms state-of-art method in terms of both accuracy and robustness. We also organize another discussion part to explore the effect of three spatial dependencies. Our contributions can be summarized as follows:

- We propose an innovative multi-scale forecasting framework called MSGNN, which provides a novel epidemic modeling view that takes multiple administrative levels into account.
- We design a multi-scale graph structure learning module to dynamically model epidemic relations at different scales, then further form a multi-scale spatio-temporal graph for epidemic forecasting.
- We design a multi-scale graph convolution network powered by a novel multi-scale information fusion scheme. This scheme distinguishes the scale-shared and scale-specific patterns, then further encodes them into representation for forecasting.

2 Related Work

Many works have put their efforts into epidemic forecasting, which can be generally categorized into three diagrams: compartmental models, time series forecasting methods, and spatio-temporal forecasting methods.

The compartmental model is a classical modeling framework in epidemiology and widely adopted in infectious disease forecasting task ([Chang et al, 2021](#); [Shuvo et al, 2020](#); [Kargas et al, 2021](#); [Qian et al, 2020](#)). The main idea of the compartmental model is to divide the population into different compartments such as S (susceptible), I (infectious), and R (recovered), and then model the transition among these compartments with differential equations ([He et al, 2020](#); [DUBEY et al, 2013](#)). In response to the COVID-19 outbreak, there emerges plenty of compartmental models specially designed according to COVID-19 virus characteristics. The main advantage of these models can be summarized to their outstanding interpretability ([Arik et al, 2020](#); [López and Rodó, 2021](#)), as they are able to produce interpretable coefficients such as infection rate, death rate, etc. However, existing compartmental models are limited to a pre-fixed basic reproduction rate, failing to learn the epidemic evolution patterns at different stages.

Time series forecasting methods reshape epidemic data into time series, turning the epidemic forecasting task into an auto-regressive problem. Common time series forecasting methods include classical statistical methods, hybrid methods and deep learning methods. The widely adopted classical statistical methods of include Auto Regressive Integrated Moving Average (ARIMA)([Maleki et al, 2020](#); [Ceylan, 2020](#)), Multi-Linear Regression (MLR)

(To et al, 2021), etc. The hybrid methods are combinations of classical methods and other methods such as machine learning (Smyl, 2020; Montero-Manso et al, 2020) and boosting trees (Chen and Guestrin, 2016). With the advancement of deep learning, some studies started to introduce neural networks such as the Long-Short Term Memory (LSTM) (Mussumeci and Codeço Coelho, 2020; Kara, 2021; Wang et al, 2020b) network to model epidemic evolution. Time series forecasting methods are capable of handling complicated temporal dependencies. However, the future epidemic trend of a specific region is not only conditioned on the local spreading, but also influenced by transmissions from other epidemic-related areas. Existing time series forecasting methods ignore the potential spatial dependencies between epidemic-related areas, leading to limited performance.

Recently, graph neural networks have attracted attention because of their strong capability in dealing with non-Euclidean space data (Derr et al, 2020; Jin et al, 2021a). With the assistance of GNN, some studies extend the time series forecasting models with spatial interactions, forming a new paradigm called spatio-temporal forecasting (Cao et al, 2020; Wu et al, 2020; Lin et al, 2020; Fang et al, 2020). This paradigm are also applied in traffic forecasting (Guo et al, 2021; Zhao et al, 2020; Yu et al, 2018) and weather forecasting (SHI et al, 2015). Also, existing studies try to leverage spatio-temporal forecasting in epidemic forecasting (Rodríguez et al, 2021; Kim et al, 2020; Jin et al, 2021b). Based on time series, these methods are capable of modeling spatial dependencies. However, due to the oversmoothing issue, their aggregation fields are limited within two hops, which means the ignorance of long-range connectivity. Moreover, the influence of multi-scale epidemic patterns are also neglected in existing epidemic modeling works.

To the best of our knowledge, our work is the first spatio-temporal forecasting study that founded on multi-scale epidemic modeling. Based on the multi-scale modeling view, we are capable of handling volatile long-range connectivity and multi-scale epidemic evolution patterns.

3 Preliminary

Epidemic signals. The epidemic development of a specific region is not only determined by local disease spreading, but also influenced by other related areas. We summarize two kinds of epidemic signals. Firstly, the short-range dependency happens between nearby areas, denoted by trans-area epidemic signal matrix A_c ; secondly, the underlying long-range connectivity, denoted by trans-regional epidemic signal matrix A_s .

Multi-scale spatio-temporal graph. Multi-scale spatio-temporal graph is a hierarchical graph containing multiple scales, denoted by $G = (V, E)$. The node set V can be further decomposed into $V = V_c \cup V_s$, where V_c and V_s respectively represent node set of micro and macro scale. Similarly, the edge set E can also be divided into $E = E_s \cup E_c$ to represent different edges at multiple

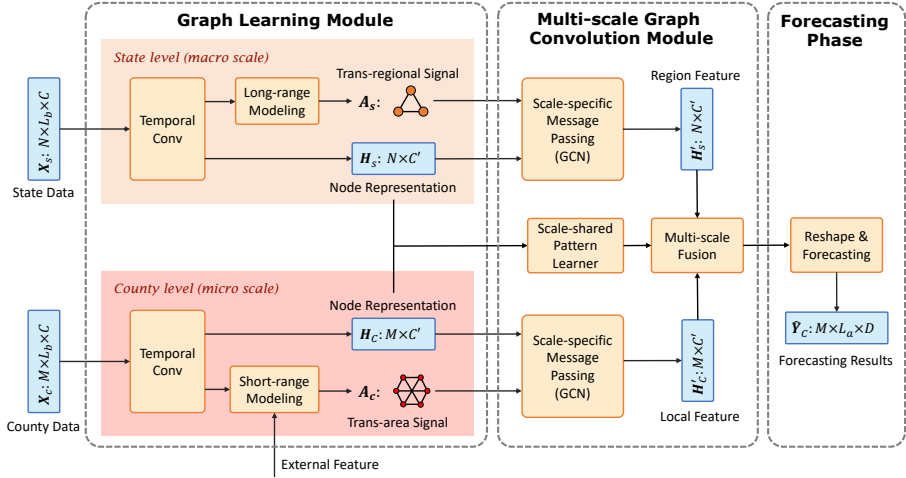


Fig. 2 Pipeline of the proposed MSGNN. The pipeline consists of two main components, i.e. the graph learning module and the multi-scale graph convolution module.

scales. Notice both V and E are time varying, which is also an important feature of spatio-temporal graph.

Infectious Disease Forecasting. Given a region i and time step t , we define the input series as $X_i(t) \in \mathbb{R}^{L_b \times C}$ as $X_i(t) = (x_{i,t-L_b+1}, x_{i,t-L_b+2}, \dots, x_{i,t})$, where L_b is the number of look-back time steps, C represents the feature dimension of input series, $x_{i,t} \in \mathbb{R}^C$ is the daily feature at time step t . The output series is similar to input series, we denote it as $\hat{Y}_i(t) \in \mathbb{R}^{L_a \times D}$, where $\hat{Y}_i(t) = (\hat{y}_{i,t+1}, \hat{y}_{i,t+2}, \dots, \hat{y}_{i,t+L_a})$, and L_a is the number of look-ahead time steps, D is the output feature dimension, $\hat{y}_{i,t+1}$ is the output value of new cases at time step $t+1$. For simplicity, we omit the time step identifier t in the rest of paper.

4 Methods

As demonstrated in Figure 2, the proposed method is a multi-scale epidemic modeling process, which contains two main components. The pipeline starts with the graph learning module, which takes the state and county level epidemic data as input. The module first conducts temporal convolution to obtain node representation, then long and short range modeling blocks are applied to produce the epidemic signals for both macro and micro scales. Based on the epidemic signals and node representations, we construct a multi-scale spatio-temporal graph. The next part is the multi-scale graph convolution module, which adopts a new multi-scale aggregation scheme. It first applies message passing to embedding scale-specific patterns, forming region and local features. Afterwards, a learner is developed to distill scale-shared patterns through graph node representations. Afterwards, the region and local features are further integrated by a newly designed multi-scale fusion block, which takes these

patterns into consideration. Finally, a forecast phase is applied to generate forecasting results.

4.1 Graph Learning Module

The adaptive graph generation module is implemented by three components, including temporal convolution blocks, long-range modeling block and short-range modeling block.

4.1.1 Temporal Convolution Block

The temporal convolution module is designed to extract local temporal features from historical epidemic time series.

For each scale, our goal is to encode the input time series X into an encoded vector H . Theoretically, the temporal convolution block can be replaced by any recurrent structures such as RNN, GRU, or LSTM. However, limited by fixed kernel size, these naive approaches fail to dynamically encode volatile epidemic dynamics. To this end, we customize a more flexible temporal convolution block based on N-Beats (Oreshkin et al, 2020) to reach our best practice. Differ from the naive N-Beats which only allows single time series as input, we additionally introduce more epidemic related series and external features, as shown in Equation 1.

$$\begin{aligned} X_s &= \text{FC}(x_{t-l_b:t}^s, d_{t-l_b:t}) \oplus \mathcal{I}_s \in \mathbb{R}^{N \times L_b \times C}, \\ X_c &= \text{FC}(x_{t-l_b:t}^c, d_{t-l_b:t}) \oplus \mathcal{I}_c \in \mathbb{R}^{M \times L_b \times C}; \end{aligned} \quad (1)$$

where $x_{t-l_b:t}$ is the input epidemic time series, $d_{t-l_b:t}$ is another time series including weekdays, holidays and date information, \mathcal{I} is the location identity embedding for each county or state. We first utilize a fully connected layer to integrate date features into original time series, then an augmentation operation is applied to introduce the location identity embedding. This customized procedure allows the block to learn epidemic patterns produced by specified time and locations, which helps boosting the performance. Next, we apply the temporal convolution scheme as follows.

$$\begin{aligned} H_s &= \text{MaxPool}[\text{TC}(X_s)] \in \mathbb{R}^{N \times C'}, \\ H_c &= \text{MaxPool}[\text{TC}(X_c)] \in \mathbb{R}^{M \times C'}; \end{aligned} \quad (2)$$

where TC is a temporal encoder based on N-Beats. We further conduct a max-pooling operation on the backcast output of temporal encoder to produce H_l as encoded feature.

4.1.2 Long-Range Modeling Block

The long-range modeling block is developed to directly capture the long-range connectivity between distant areas. This block takes the output of macro scale temporal convolution block H_s as input, and produces an adjacency matrix A_s representing the connectivity between different states.

For specified states $l, k \in V_s$, we denote the pairwise connectivity as $[A]_s^{l,k}$. To dynamically measure the volatile long-range connectivity, we choose the real-time node representation H_l, H_k as the key factor, which can be expressed as Equation 3.

$$[A]_s^{l,k} = f [\theta_s^T \cdot \text{Concat}(H_l, H_k)]; \quad (3)$$

where $\theta_s^T \in \mathbb{R}^{2 \times C'}$ is trainable mapping vectors, f is the activation function. The idea of long-range connectivity modeling is mapping concatenated features into an adjacency edge scalar value. Due to the evolving node representations, the connectivities are also self-adjusted according to the real-time epidemic situation. In this block, the obtained long-range connectivity is determined by epidemic relations among different states. For those distant but epidemic-related areas, these newly introduced long-range connectivities can create a directly connected graph edge, thus breaking the spatial limitations.

4.1.3 Short-Range Modeling Block

Aside from the long-range connectivity, we also elaborate on another trans-regional signal called short-range dependency. The short-range dependency are estimated at micro scale, which depicts the fine-resolution geographic topology for county level. Moreover, because of finer resolution, the short-range dependencies may be affected by other factors, such as geographic distance, administration boundary, etc.

For counties i, l in micro scale, we denote the short-range dependency as $[A]_c^{i,l}$. Differ from the long-range connectivity, we introduce extra signals to assist constructing the adjacency matrix, which can be expressed as Equation 4.

$$[A]_c^{i,j} = f [\theta_c^T \cdot \text{Concat}(H_i, H_j, \mathcal{I}_i, \mathcal{I}_j)] + \frac{1}{\sqrt{\delta_{i,j}}}; \quad (4)$$

where $\theta_c^T \in \mathbb{R}^{4 \times C'}$ is a trainable mapping vector, f is the activation function, \mathcal{I} is the identity embedding for each location, and $\delta_{i,j}$ is the geographic distance between county i and j . Apart from measuring epidemic relation, we additionally add the identity information to introduce the administration boundary information, which means counties in the same state will create stronger short-range dependency. Moreover, since the micro scale features narrower spatial effects, we add the geographic distance factor λ to express the spatial limitations. Finally, to avoid noisy and redundant graph structure, we utilize *ReLU* as the activation function to completely shutdown the adjacency edge between irrelevant counties.

4.2 Multi-scale Graph Convolution Module

After the graph learning module, we obtain a new multi-scale spatio-temporal graph where each node represents regions and edges represent the epidemic

signal. To model the epidemic evolution, a natural idea is to use graph convolution network to aggregate information. To this end, we propose the multi-scale graph convolution module. This module is composed by scale-specific message passing blocks, scale-shared patterns learner and a multi-scale fusion block, which forms a novel multi-scale information fusion scheme. In this module, the learned multi-scale spatio-temporal graph serves as the input, and the module outputs an epidemic representation for final forecasting.

4.2.1 Scale-specific Message Passing Block

To deal with the scale-specific epidemic patterns, we implement the messaging passing block to deal with the epidemic information within single scale. The block takes the node representation H and adjacency matrix A as input. However, it is worth noting that A is a diagonal-dominant matrix, which means the self-loops are much stronger than other connections. Since self-loops may do harm to the information aggregation between adjacent nodes (Kipf and Welling, 2017a), we obtain new adjacency matrix $\tilde{A}_s \in \mathbb{R}^{N \times N}$ and $\tilde{A}_c \in \mathbb{R}^{M \times M}$ by zeroing the diagonal and performing normalization, as shown in Equation 5:

$$\hat{A} = A - \text{diag}(A), \quad \tilde{A} = \hat{D}^{-\frac{1}{2}} \hat{A} \hat{D}^{-\frac{1}{2}}; \quad (5)$$

where \hat{D} is the degree matrix of adjacency matrix \hat{A} . Then, we apply graph convolution at micro scale and macro scale respectively, so as to generate the local feature $H'_c \in \mathbb{R}^{M \times C'}$ and region feature $H'_s \in \mathbb{R}^{N \times C'}$ as Equation 6:

$$\begin{aligned} H'_c &= \text{GCN}(\tilde{A}_c, H_c) = \tilde{A}_c f(\tilde{A}_c H_c U_1) U_2 \in \mathbb{R}^{M \times C'}; \\ H'_s &= \text{GCN}(\tilde{A}_s, H_s) = \tilde{A}_s f(\tilde{A}_s H_s U_3) U_4 \in \mathbb{R}^{N \times C'}; \end{aligned} \quad (6)$$

where $U_1, U_2, U_3, U_4 \in \mathbb{R}^{C' \times C'}$ are trainable weight matrix, f is the activation function. Here we apply a two-layer GCN for both micro scale and macro scale. Note that the aggregation weight matrix for micro and macro scales are different, allowing the model to learn different epidemic patterns specified to certain scales. Through this way, the epidemic information are passed through multi-scale graph, which generates local features at micro scale and region features at macro scale.

4.2.2 Scale-shared Pattern Learner

In this block, we utilize the obtained node representation to measure the scale-shared epidemic evolution pattern between state and county levels. Here we first construct a transfer matrix to identify the administrative affiliation between counties and their belonging states, denoted as $Tran \in \mathbb{R}^{M \times N}$ as Equation 7:

$$[Tran]_{i,l} = \begin{cases} \frac{1}{N(i)}, & \text{if county } i \text{ affiliated to state } l, \\ 0, & \text{else;} \end{cases} \quad (7)$$

where $\mathcal{N}(l)$ is the number of counties that belongs to state l . Next, we obtain the multi-scale epidemic patterns from different scales. For macro scale, we directly use the node representation as the epidemic patterns. For micro scale, We aggregate the node representations of counties that belong to the same state, as shown in the Equation 8:

$$H_c^{Tran} = (Tran)(H_c) \in \mathbb{R}^{N \times C'} \quad (8)$$

According to the transfer matrix $Tran$, the produced H_c^{Tran} is an averaged representation from all counties, e.g. the l -th row of H_c^{Tran} refers to the averaged representation of all counties from state l .

Since transfer representation H_c^{Tran} and state representations H_s are collected at different scales, they have different epidemic evolution patterns. To mine the latent scale-shared patterns, we use the Temporal Attention (Feng et al, 2017) to capture the cross-scale temporal correlations, as shown in Equation 9:

$$E = ((H_s)^T U_5) U_6 (H_c^{Tran} U_7 + \beta)^T \in \mathbb{R}^{N \times N} \quad (9)$$

where $U_5, U_7 \in \mathbb{R}^{N \times C'}$ and $U_6 \in \mathbb{R}^{N \times N}$ are trainable weight matrix. Because of the dynamic node representations in spatio-temporal graph, the correlation matrix E also changes along with epidemic evolution.

4.2.3 Multi-scale Fusion Block

To incorporate local and region representations for final forecasting, we develop the multi-scale fusion block to comprehensively consider scale-shared and scale-specific patterns. We first devise a scheme to extract scale-shared epidemic representations from macro scale:

$$[E']_{i,j} = \frac{\exp([E]_{i,j})}{\sum_{j \in (0,N)} \exp([E]_{i,j})}, \quad (10)$$

$$Att(H'_s) = E' H'_s$$

The scale-shared pattern is extracted by correlation matrix E . Moreover, we further connect the scale-specific pattern H'_c to the scale-shared part by Equation 11:

$$H_{out} = \text{Concat} [Att(H'_s), H'_c] \in \mathbb{R}^{2C'} \quad (11)$$

4.3 Forecasting Module

The forecasting module is implemented to forecast based on the output of multi-scale graph convolution network.

To generate final forecasting results, we use a weight matrix $\theta_f \in \mathbb{R}^{L_a \times 2C'}$ to produce the final forecast \hat{Y}_i of county i with L_a time steps ahead. During

the training, we use the mean squared error of \hat{Y} and Y to form the loss function. For ground truth values $Y = \{y_{(t+1)}, \dots, y_{(t+L_a)}\}$

$$\begin{aligned} \hat{Y} &= \theta_f \cdot H_{out}, \\ loss &= MAE(\hat{Y}, Y) \\ &= \frac{\sum_{i=1}^{L_a} \sum_{j=1}^N |(\hat{y}_{(t+i)}^j - y_{(t+i)}^j)|}{L_a * N}; \end{aligned} \quad (12)$$

At the end of the method section, we summarize the algorithm of proposed MSGNN as shown in Algorithm 1.

Algorithm 1 The MSGNN model for epidemic forecasting.

Require: The historical epidemic time series for micro scale (e.g. the county level in the US): $X_c = \{x_{t-L_b+1}^c, x_{t-L_b+2}^c, \dots, x_t^c\} \in \mathbb{R}^{M \times L_b \times C}$;

Require: The historical epidemic time series for macro scale (e.g. the state level in the US): $X_s = \{x_{t-L_b+1}^s, \dots, x_t^s\} \in \mathbb{R}^{N \times L_b \times C}$;

- 1: Get the node representations of micro scale $H_c \in \mathbb{R}^{M \times C'}$ from X_c by temporal convolution blocks;
 - 2: Get the node representations of macro scale $H_s \in \mathbb{R}^{N \times C'}$ from X_s by temporal convolution blocks;
 - 3: Get trans-area epidemic signal matrix $A_c \in \mathbb{R}^{M \times M}$ from temporal feature H_c ;
 - 4: Get trans-regional epidemic signal matrix $A_s \in \mathbb{R}^{N \times N}$ from temporal feature H_s ;
 - 5: Get region feature H'_s by applying message passing on graph (A_s, H_s) ;
 - 6: Get local feature H'_c by applying message passing on graph (A_c, H_c) ;
 - 7: Get the combined feature H_{out} from H'_c, H'_s, E by multi-scale fusion block;
 - 8: Get forecasting *Output* of MSGNN based on H_{out} ;
 - 9: **return** *Output*;
 - 10: Calculate the loss of MSGNN.
-

5 Experiment

To validate the infectious disease modeling ability, we evaluate the proposed model by forecasting the COVID-19 epidemic, the latest and one of the most prevalent infectious diseases for decades. We elaborate the experiments mainly on the COVID-19 Forecast Hub ¹ (hereon referred as *The Hub*), an official global challenge raised by United State Centers for Disease Control and Prevention (CDC) to accommodate weekly epidemic forecasting results from international groups. Since *The Hub* released the forecasting results of all submitted models, we can easily get access to the performance of competitors and make comparison.

¹<https://covid19forecasthub.org>

5.1 Experimental Settings

5.1.1 Data

For COVID-19 epidemic data, we leverage daily reported cases and deaths from the Johns Hopkins University Center for Systems Science and Engineering (JHU CSSE) as the gold-standard data ². The dataset collects incident cases and deaths from both state and county level in the United State. Following the location set defined by *The Hub*, our experiment is conducted on 50 states and 3142 subordinated counties. The dataset date range is set from March 1, 2020 to July 1, 2021. The detailed statics are shown in Table 1.

Table 1 Detailed statics of the JHU CSSE dataset.

		# location	# dates	Min	Max	Ave
US-State	confirmed	50	487	0	73854	1660
	deaths	50	487	0	4417	450
US-County	confirmed	3142	487	0	34497	62
	deaths	3142	487	0	761	15

For geographical data, we directly use the geographic information in the JHU CSSE dataset, which contains the latitude and longitude of all regions in the US. The geographic data provides the state adjacency and county adjacency relationship information in the United State.

For population data, we use the state and county population information (2019) in the United State to perform normalization to both confirmed and deaths data.

5.1.2 Evaluation Metrics

As to evaluation metrics, we keep accordance with the requirements on *The Hub*. Since the daily reported cases may be rather vibrating and unstable, we leverage weekly reported confirmed cases as our primary forecasting target. Our evaluation range is from February 2021 to July 2021. On each Sunday, we generate a forecasting result including one week, two weeks and three weeks ahead. In the five months evaluation period, we provides tens of forecasting results and calculating the performance indicators using three metrics, i.e. mean average error (MAE), mean average percent error (MAPE) and root mean square error (RMSE), which can be calculated as Equation 13:

²<https://github.com/CSSEGISandData/COVID-19>

$$\begin{aligned}
 MAE &= \frac{1}{n} \sum_{i=1}^n |\hat{y}_i - y_i|, \\
 MAPE &= \frac{100\%}{n} \sum_{i=1}^n \left| \frac{\hat{y}_i - y_i}{y_i} \right|, \\
 RMSE &= \sqrt{\frac{1}{n} \sum_{i=1}^n (\hat{y}_i - y_i)^2};
 \end{aligned} \tag{13}$$

where \hat{y} is the forecasting output, y is the ground truth value, n is the location number. As shown in Equation 13, the MAE measures the absolute difference between two values, averaged by the location number. The MAPE is also an error measure of two values in percentage terms. The RMSE is another frequently used metric, it represents the square root of the differences between predicted values and observed values. All the three metrics range in $[0, +\infty]$ and smaller values are better.

For the whole evaluation period with over ten weeks, we conduct two experiments. We first average these per-week metrics to produce the main evaluation results containing MAE, MAPE, and RMSE. Moreover, we design another experiment called per-week evaluation to help understand the statistical distribution of forecasting results, so as to test the robustness of models. Besides, to keep consistency with the evaluation standard on *The Hub*³, we calculate the three metrics on the most 500 populous counties in the US (@500), i.e. $n = 500$ in Equation 13. Furthermore, we utilize another relatively small dataset consisting of the most 100 populous counties (@100), i.e. $n = 100$ in Equation 13 to comprehensively evaluate the performances of all models.

5.2 Baselines

To serve as the baselines, we choose a broad range of competitive COVID-19 forecasting models reported on *The Hub*. It is worth noting that most of the models on *The Hub* do not have their codes released, so instead of reproducing their forecasting results, we directly take their submitting result on the website. Furthermore, considering the frequency of submission and target forecasting location sets are varied, we set the filtering criteria as follows: candidate models should produce complete weekly outputs ranging from May, 2020 to July, 2021, also, the model must provide epidemic forecasting output of more than 3000 counties for full evaluation. We select 10 models satisfying the requirements as follows:

- **Microsoft-DeepSTIA** (Zheng et al, 2021): A deep spatio-temporal network, proposed by Microsoft Research.
- **USC-SI.kJalpha** (Srivastava et al, 2020): A SIR model with vaccines and multiple variants, proposed by University of South California.

³[https://covid19forecasthub.org/eval-reports/#Incident_Case_Forecasts_\(county\)](https://covid19forecasthub.org/eval-reports/#Incident_Case_Forecasts_(county))

- **UVA-Ensemble** (Adiga et al, 2021): An ensemble model containing auto-regressive approach, SEIR approach and machine learning approach, proposed by University of Virginia.
- **Google_Harvard-CPF** (Arik et al, 2020): A SEIR model fitted by machine learning approach, proposed by Google Cloud AI.
- **CEID_Walk**⁴: A random walk model without drift, proposed by University of Georgia.
- **IowaStateLW-STEM** (Wang et al, 2020a): A quasi-likelihood approach via the penalized spline approximation, proposed by Iowa State University.
- **JHUAPL-Bucky** (Panaggio et al, 2022): A spatial compartment model using public mobility data, proposed by Johns Hopkins University.
- **CU-nochange** (Pei and Shaman, 2020): A metapopulation county-level SEIR model, proposed by Columbia University.
- **COVIDhub-Ensemble** (Ray et al, 2020): An ensemble model containing the best performed models on *The Hub*, proposed by the CDC.

Due to the limit of space, more detailed information of compared models can be found at COVID-19 Forecast Hub official website⁵.

5.3 Implementation Details

All of our implementations run on a server with an Intel Xeon Platinum 8369B @2.9GHz CPU and a single NVIDIA RTX 2070 Super GPU. To eliminate the data bias originated by demographic differences, we normalize all the data by population factor, encouraging the model to learn the common epidemic patterns sharing across different administrative scales. We set our model to look back 14 days, i.e. we begin training at the beginning of each week with features of last week, producing the inferences for the next week. Moreover, to allow an early stop, we take the latest data of all locations as the validation set. Finally, for the robustness of our proposed model, we utilize different random seeds for training, then averaged the final forecasting result from different seeds. For the N-Beats in temporal convolution module, we set its dimension as 32. As for the graph convolution module, we set the network dimension as 64 with 2 layers, the aggregation type is Max-Pooling, and the node and edge dimensions are 4. The batch size is set as 4 and the learning rate is set as 1e-3. For the graph optimization, we utilize the mini-batch training techniques, the batches are sampled from the whole graph in a certain time period, forming a new sub-graph. In practice, we utilize the random-walk sampling techniques to form the new sub-graphs. Moreover, all the sampled dates are randomly shuffled to avoid information leakage.

5.4 Main Evaluation Results

The main evaluation result is reported in Table 2, with best results highlighted in bold and second best highlighted in underline. The evaluation is divided into

⁴<https://github.com/e3bo/random-walks>

⁵<https://zoltardata.com/project/44>

Table 2 A summary of main evaluation results. Best results are highlighted in bold and second best results are highlighted by underlines.

Dataset		@500			@100		
Method	Metric	1wk	2wk	3wk	1wk	2wk	3wk
Microsoft-DeepSTIA	MAE	139.0	506.7	988.4	374.5	1414.4	2628.7
	MAPE	0.425	0.455	0.607	0.392	0.461	0.604
	RMSE	341.3	<u>980.0</u>	<u>1808.5</u>	677.2	<u>1992.7</u>	3911.9
USC-SLkJalpha	MAE	141.1	541.6	1045.5	<u>343.1</u>	1440.3	2781.6
	MAPE	0.430	0.546	0.733	<u>0.369</u>	0.535	0.732
	RMSE	366.0	1072.7	2015.6	650.1	2081.0	3935.7
UVA-Ensemble	MAE	159.7	587.6	1071.6	411.3	1570.6	2866.9
	MAPE	0.451	0.591	0.730	0.443	0.598	0.739
	RMSE	418.1	1073.6	1873.3	822.1	2179.2	3842.6
Google_Harvard-CPF	MAE	178.2	685.7	1211.8	465.6	1917.1	3346.8
	MAPE	0.456	0.627	0.738	0.368	0.623	0.767
	RMSE	408.1	1352.7	2283.2	777.9	2794.2	4718.0
CEID_Walk	MAE	155.4	485.1	969.2	409.3	<u>1390.2</u>	2594.6
	MAPE	0.492	<u>0.443</u>	<u>0.593</u>	0.438	<u>0.447</u>	<u>0.573</u>
	RMSE	371.8	<u>1021.5</u>	1724.7	742.6	2016.2	3931.2
IowaStateLW-STEM	MAE	321.5	694.4	1240.5	929.0	1870.2	3316.7
	MAPE	0.729	0.550	0.644	0.654	0.554	0.669
	RMSE	1091.4	1481.9	2284.9	2312.3	3054.7	4684.4
JHUAPL-Bucky	MAE	210.5	582.1	1067.3	543.1	1501.9	2813.2
	MAPE	0.550	0.614	0.746	0.458	0.542	0.715
	RMSE	530.8	1220.1	2012.1	972.7	2154.2	3844.2
CU-nochange	MAE	135.1	577.3	1080.3	352.5	1585.7	<u>2590.7</u>
	MAPE	<u>0.347</u>	0.544	0.710	<u>0.285</u>	0.543	<u>0.585</u>
	RMSE	327.7	1119.2	2006.1	643.4	2304.4	4144.3
COVIDhub-ensemble	MAE	<u>132.2</u>	550.2	1040.5	343.8	1482.2	2808.6
	MAPE	<u>0.400</u>	0.491	0.650	0.339	0.481	0.645
	RMSE	<u>312.3</u>	1035.9	1878.5	<u>599.5</u>	2108.6	3822.6
MSGNN (Ours)	MAE	121.3	<u>502.2</u>	959.6	321.5	1360.4	2588.5
	MAPE	0.340	0.439	0.584	0.283	0.432	0.571
	RMSE	302.2	977.8	1867.8	594.8	1990.5	<u>3840.9</u>

two datasets, i.e. @500 and @100. For each dataset, we set three forecasting horizons containing one week ahead, two weeks ahead and three weeks ahead, then further calculating their evaluation metrics containing MAE, MAPE and RMSE. All metrics are computed on the US county level, then further averaged to obtain main evaluation results. The same result processing strategies are also applied to other baselines.

As shown in Table 2, our model has superior performance over any other baselines. In most cases, our proposed model produces the best results. For

example, when we set the forecasting horizon as one week ahead, our proposed model achieved the lowest MAE, MAPE and RMSE in terms of both @500 and @100 datasets, the best performed baseline forecasting MAE is 132.2 and our proposed model reaches 121.3, bringing in up to 10% of the performance gain. Moreover, when the forecasting horizon is set as two weeks and more, the proposed model still manages to outperforms the state-of-art methods in terms of MAPE and MAE. Despite the fact that in some cases other baselines achieve better result, our model still manages to achieve the second best score.

It is also worth noting that for all models, the forecasting accuracy drops when the forecasting horizon becomes longer. For example, the CU-nochange model reaches 0.347 and 135.1 for MAPE and MAE, which is a pretty competitive result in 1-week forecasting scenario. However, when broadening the forecasting horizon, its performance drops sharply to 0.710 and 1080.3. Similarly, the USC-SI.kJalpha model outperforms most of the baselines in short term forecasting, while producing much poorer results in long term forecasting. Taking all forecasting horizons into consideration, we can observe that the proposed MSGNN still has strong performance. Only for the forecasting in next three weeks, the RMSE metric of MSGNN is relatively larger than other baselines, such as CEID_Walk and COVIDhub-ensemble. While for all other cases, the proposed model is the best performing model in terms of averaged accuracy.

5.5 Per-week Evaluation Results

Aside from inspecting the main evaluation result, we also notice significant variations in performance across different weeks. Some baseline models may suffer a great performance degradation when facing challenging epidemic patterns, such as sharp increments in confirmed cases, unstable mortality curves, etc. Since these challenging epidemic patterns are widespread in epidemic outbreaks, the sensitivity to these patterns may exert a dramatic negative impact on model robustness.

To this end, we designed another experiment called per-week evaluation experiment. In this experiment, we collect forecasting error metrics for each model every week from February 2021 to July 2021, and further visualize their distributions to help validate robustness of both proposed model and its competitors.

As illustrated in Figure 3, the per-week evaluation results of the proposed model is still competitive in terms of MAE, MAPE and RMSE metrics. Our proposed model outperforms other baselines in three perspectives. Firstly, the median value of the proposed model is low. Compared with CEID_Walk, one of best performed baselines in averaged evaluation experiments, our proposed model reached significantly lower error medians in terms of MAE, MAPE and RMSE. Secondly, the proposed model produces much smaller performance variations. Other competitive models such as Microsoft-DeepSTIA and COVIDhub-ensemble feature larger variations in performance, which means their error distributions are scattered. On the contrary, the proposed model

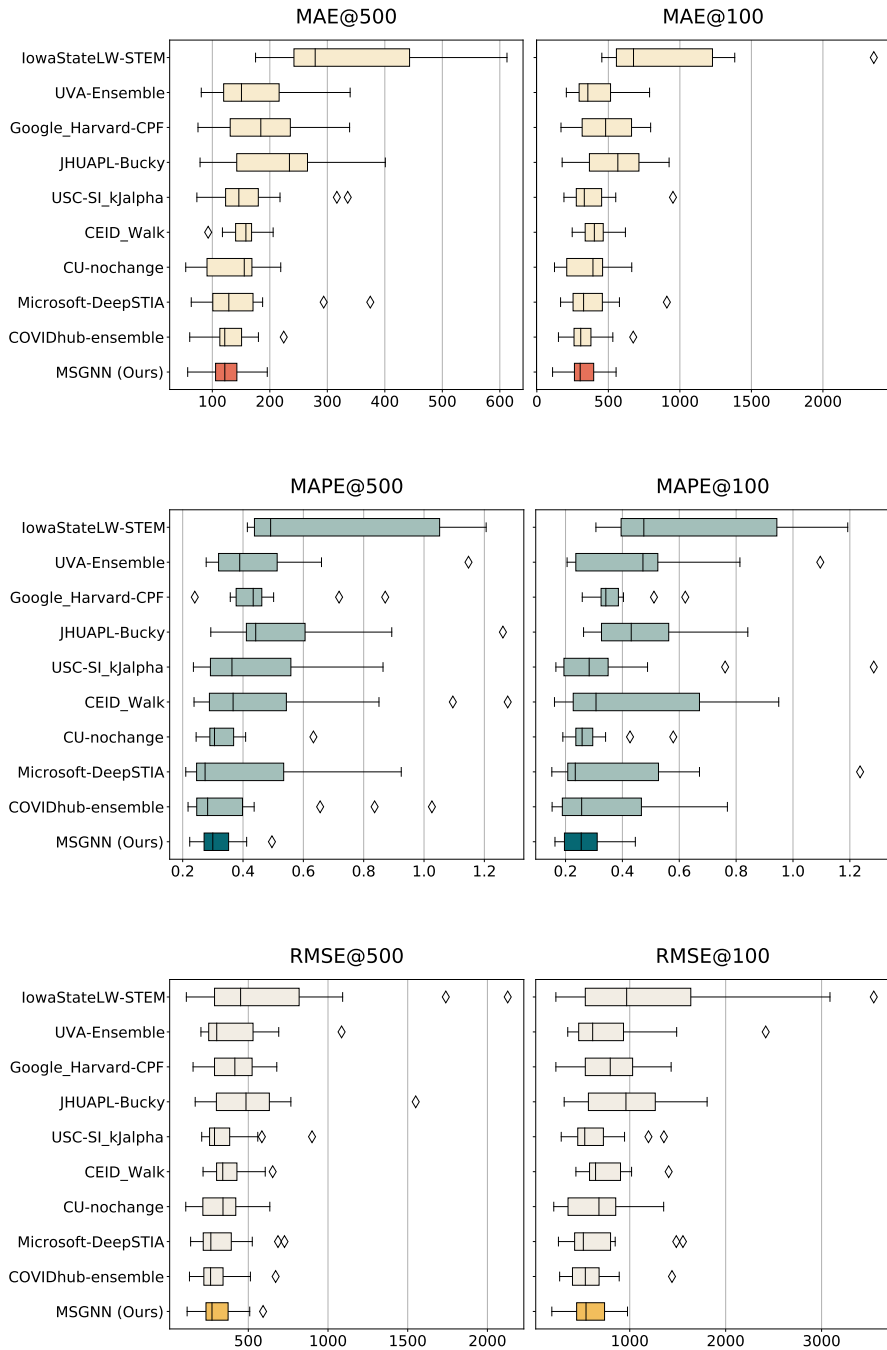


Fig. 3 The per-week evaluation results for model robustness experiments, all the results are presented as box plots.

has smaller rectangle size and produces stabler forecasting results compared to other competitors. Finally, MSGNN produces less outliers. The hollow diamonds represent the outliers, whose statistic values are extremely high or extremely low. More outliers will do harm to model's forecasting robustness, leading to lower reliability. Combining the box plots of MAE, MAPE and RMSE, we observe that the total number of outliers produced by MSGNN is the least among all the compared baseline models.

All the observations prove that when facing challenging epidemic patterns, the proposed model performs more robust than all the baseline models. In summary, the proposed model is the most competitive model producing not only accurate, but also robust epidemic forecasting result.

5.6 Ablation Study

To verify the effectiveness of each component in proposed model, we conduct a comprehensive ablation study, whose result is shown in Table 3. All the experiments are conducted on both @500 and @100 dataset and the results are obtained by averaging the outputs of forecasting 1-week ahead, 2-weeks ahead and 3-weeks ahead. The original version of our proposed model is MSGNN. To further prove the effectiveness of our model, we add another two best performed baselines, i.e. CEID_Walk and COVIDhub-ensemble for comparison.

5.6.1 Effect of the multi-scale modeling

To evaluate the contribution of the multi-scale structure, we create the first variant:

MSGNN-w/o-ms. MSGNN-w/o-ms is a variant which models epidemic only in county level. To achieve so, we completely remove the additional state level in proposed model, downgrading it to a single-scale spatio-temporal model. Under this circumstance, the model is only accessible to the county level epidemic patterns, thus inevitably leading to worse performance. It can be observed in Table 3 that MSGNN-w/o-ms variant produces the worst result among all baselines and variants on both @500 and @100 datasets, which indicates the importance of multi-scale modeling in epidemic forecasting. The reasons why the multi-scale modeling is important could be that without the assistance of information from upper administrative level, the model can only attend to their closest neighbours for information aggregations, ignoring the latent long-range connectivity.

5.6.2 Effect of graph learning module

To understand the role that graph learning module plays in epidemic modeling, we design two variants excluding the graph learning procedures.

MSGNN-w-GCN. In this variant, we use graph convolution network to replace the graph learning module, i.e. we exclude the dynamic multi-scale spatio-temporal graph and directly use the static geographical distance graph to get the forecasting result, thus forming a naive graph convolution network

Table 3 A summary of ablation study results, based on @100 and @500 datasets, averaged by 1-week, 2-weeks, 3-weeks ahead forecasting MAPE.

Dataset	@100		@500	
Metric	MAPE	Relative Increments	MAPE	Relative Increments
CEID-Walk	0.479	+5.1%	0.509	+4.9%
COVIDhub-ensemble	0.489	+6.1%	0.514	+6%
MSGNN	0.428	-	0.454	-
MSGNN-w/o-ms	0.509	+8.1%	0.515	+6.1%
MSGNN-w-GCN	0.470	+4.2%	0.491	+3.7%
MSGNN-w-GAT	0.479	+5.1%	0.489	+3.5%
MSGNN-w/o-fusion	0.467	+3.9%	0.475	+2.1%

(Kipf and Welling, 2017b). According to the experiment result, the variant performs obviously worse than the original model, which indicates the the dynamic spatio-temporal graph contributes positively to epidemic modeling, enabling the model to dynamically attend to the most relevant regions. Moreover, when applying the naive graph convolution network, the model fails to capture those time-varying dependencies. This is caused by static geographic information serves as the dominant element in spatio-temporal modeling instead of dynamic epidemic interactions.

MSGNN-w-GAT. Aside from utilizing a static graph, we also develop a variant using graph attention mechanism to construct spatio-temporal graphs. In this variant, we replace the adaptive generation module completely with graph attention network (Velickovic et al, 2018). As shown in the experiment result, our model outperforms this variant, which proves the effectiveness of self-adaptive adjustment mechanism. Although the graph attention mechanism is capable of capturing part of the dynamic spatial dependencies, however, it fails to take the latent long range spatial dependencies into consideration, leading to limited performance.

The two variants mentioned above prove the effectiveness of the proposed adaptive graph generation module. With the specifically designed graph learning module, MSGNN can balance both temporal signals and spatial signals. Moreover, the self-adaptive adjustment mechanism assists model distinguishing the most epidemic relevant features, avoiding introducing irrelevant noises.

5.6.3 Effect of multi-scale graph convolution module

MSGNN-w/o-fusion. In this variant, we remove the multi-scale fusion blocks and directly concatenate local and region features to form the final representations for forecasting. Therefore, this variant is not accessible to scale-specific and scale-shared epidemic patterns. Due to the missing multi-scale epidemic patterns, the performance of this variant is limited compared to the original version. However, it is important to note that although the variant achieves inferior performance over the proposed model, it still outperforms the

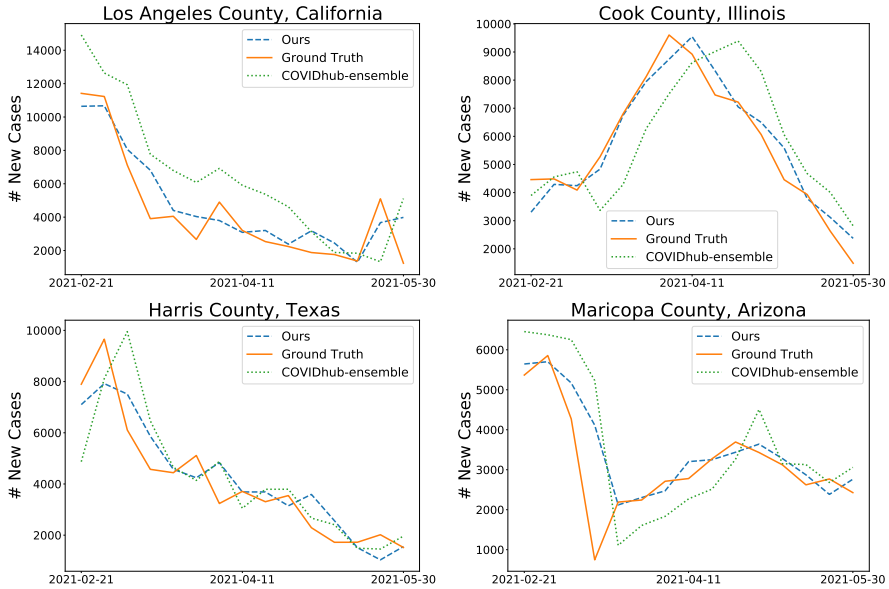


Fig. 4 Case studies for four counties with the largest population within a fifteen weeks evaluation period.

state-of-art baselines including CEID.Walk and COVIDhub-ensemble, indicating the multi-scale spatio-temporal graph helps modeling the epidemics better.

5.7 Case Study

To intuitively understand the evaluation experiments mentioned above, we specifically select four US counties with the largest population to visualize the case study, i.e. Los Angeles County of California, Cook County of Illinois, Harris County of Texas and Maricopa County of Arizona, which are distributed in different parts of the United State. We compare their true incident cases with the forecasting results produced by MSGNN and one of the best performed baseline COVIDhub-ensemble. It is noticeable that COVIDhub-ensemble is an embedding model officially proposed by United State Centers for Disease Control and Prevention (CDC), which comprehensively takes all of the forecasting result from other teams into consideration.

The result is shown in Figure 4. We can observe that our model still outperforms the COVIDhub-ensemble in all the counties for comparison, producing more accurate and stable forecasting results. In Los Angeles county and Harris county, the trend of ground truth is single and obvious, and the forecasting curve produced by MSGNN fits the ground truth curves better, which means the proposed model achieves better accuracy than COVIDhub-ensemble model. While in the Harris county and Maricopa county, the epidemic trend features more complicated patterns, e.g. larger slope of curves, more slope

turning corners, etc. These complex patterns challenge the models' forecasting robustness. It is obvious that the COVIDhub-ensemble model performs poorly with these patterns, where the produced curves are unstable and keep vibrating. Although the proposed MSGNN is also affected by these patterns, it still manages to fit the ground truth in most of the evaluation dates, showing stronger robustness than its competitors. Generally, the overall performance of MSGNN wins more cases than the COVIDhub-ensemble model does.

6 Discussion: Interpretability Study

To fully understand the interpretability of our proposed model, in this section, we take a deeper inspect on trans-area and trans-regional epidemic signals produced by graph learning module. Due to the coupled model structure, previous GNN-based methods fail to study model interpretability, which harms forecasting result's credibility. On the contrary, the proposed MSGNN is decoupled into two modules. We can easily study the model's interpretability by inspecting the intermediate output. As the epidemic signals fully control all message passing in the following module, we select the trans-regional and trans-area epidemic signals (i.e. the output of graph learning module), and study the internal relationship between epidemic evolution and these signals.

We visualize the evolution of epidemic signals alongside national incident numbers. Since our customized graph learning module can dynamically adjust the graph edges based on current epidemic situations, so we directly measures the strength of dependencies through edge weights, where larger edge weights correspond to more active signals. We record all the edge weights produced by a fully trained MSGNN for each forecasting date and present the results in two line charts. as shown in Figure 5.

Firstly, for long-range connectivity, we can observe that the signals tend to become activated before next wave of sharply increasing new cases. For example, the first peak of activated signals appears in March 2020, which is followed by a rapidly increasing wave of incident cases in April 2020. This kind of pattern is not unique and recur in May 2020, June 2020, October 2020 and February 2021. By aligning the evolution of long-range connectivity with national incident curve, we suggest this interesting pattern reflects the potential transmission process between distant regions. The more active trans-regional epidemic signals indicate the more benefits of spatial signals in epidemic forecasting, which also implies more distant transmissions in the physical world.

Secondly, it is obvious that the active period of short-range dependency almost covers the peak of long-range connectivity. Especially since January 2021, the trans-area signals have much more distinct peak values than long-range connectivity. We conjectured that as the pandemic is gradually controlled in 2021, the large scale nation-wise transmissions were successfully suppressed, leading to inactivated long-range connectivity signals. However,

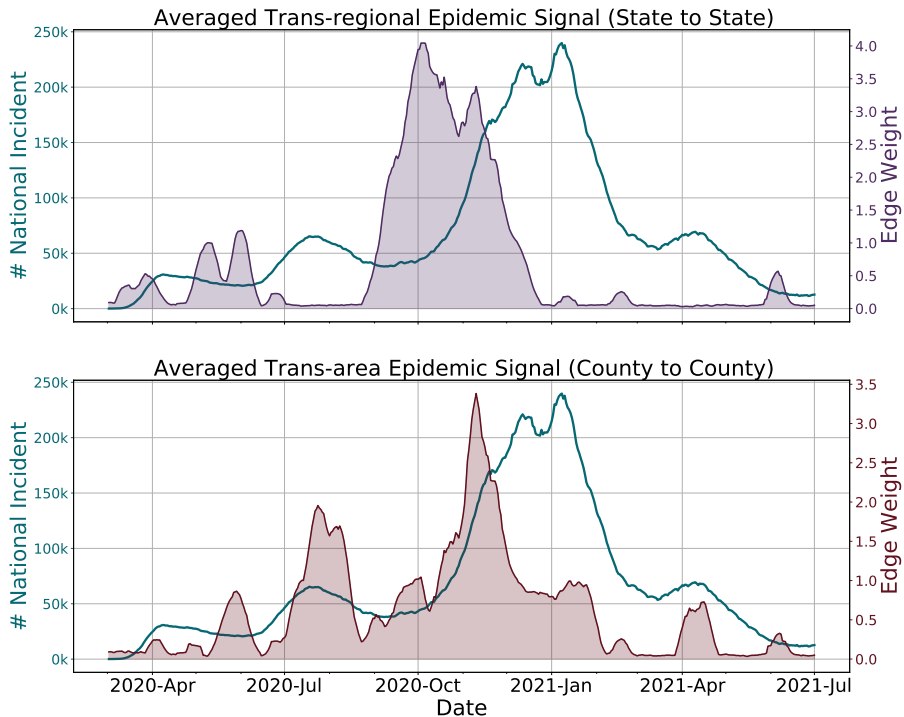


Fig. 5 The evolution of spatial dependencies produced by MSGNN (plotted as colored and filled lines) alongside with weekly national incident number (plotted as dark line).

the local epidemic transmissions still exist and forms active short-range epidemic signals. Hence, we suggest the short-range dependency indicates the local transmission process among neighbouring areas.

In summary, the proposed MSGNN has some interpretable capacities as it explicitly shows how epidemic transmit at different spatial scales. On one hand, the learned epidemic signals help modeling epidemic better and ensure the credibility of forecasting result. On the other hand, it also installs confidence in end-users such as policy makers and citizens.

7 Conclusions

In this paper, we propose Multi-scale Spatio-temporal Graph Neural Network (MSGNN) for epidemic forecasting. Specifically, we design a novel multi-scale epidemic modeling method. On one hand, we devise a graph learning module to directly captures long-range connectivity and integrate them into a multi-scale spatio-temporal graph. On the other hand, we customized a multi-scale graph convolution module, which adopts a novel information aggregation scheme. The scheme allows us to distinguish both scale-specific and scale-shared epidemic patterns, which gives rise to multi-scale modeling. Extensive experiments are conducted and the results demonstrate the capacity of MSGNN

from multiple dimensions, including the forecasting accuracy, robustness and forecasting interpretability.

Declarations

Funding. This work was supported by National Key Research and Development Project (No.2020AAA0106200), the National Nature Science Foundation of China under Grants (No.61936005, 61872424), the Natural Science Foundation of Jiangsu Province (Grants No.BK20200037 and BK20210595).

Conflict of interests. The authors have no conflict of interest to declare that are relevant to the content of this article.

References

- Adiga A, Wang L, Hurt B, et al (2021) All models are useful: Bayesian ensembling for robust high resolution covid-19 forecasting. In: Proceedings of the 27th ACM SIGKDD Conference on Knowledge Discovery & Data Mining. Association for Computing Machinery, New York, NY, USA, KDD '21, p 2505–2513, <https://doi.org/10.1145/3447548.3467197>, URL <https://doi.org/10.1145/3447548.3467197>
- Arik S, Li CL, Yoon J, et al (2020) Interpretable sequence learning for covid-19 forecasting. In: Larochelle H, Ranzato M, Hadsell R, et al (eds) Advances in Neural Information Processing Systems, vol 33. Curran Associates, Inc., pp 18,807–18,818, URL <https://proceedings.neurips.cc/paper/2020/file/d9dbc51dc534921589adf460c85cd824-Paper.pdf>
- Cao D, Wang Y, Duan J, et al (2020) Spectral temporal graph neural network for multivariate time-series forecasting. In: Larochelle H, Ranzato M, Hadsell R, et al (eds) Advances in Neural Information Processing Systems, vol 33. Curran Associates, Inc., pp 17,766–17,778, URL <https://proceedings.neurips.cc/paper/2020/file/cdf6581cb7aca4b7e19ef136c6e601a5-Paper.pdf>
- Ceylan Z (2020) Estimation of covid-19 prevalence in italy, spain, and france. *Science of The Total Environment* 729:138,817. <https://doi.org/https://doi.org/10.1016/j.scitotenv.2020.138817>, URL <https://www.sciencedirect.com/science/article/pii/S0048969720323342>
- Chang S, Wilson ML, Lewis B, et al (2021) Supporting covid-19 policy response with large-scale mobility-based modeling. In: Proceedings of the 27th ACM SIGKDD Conference on Knowledge Discovery & Data Mining. Association for Computing Machinery, New York, NY, USA, KDD '21, p 2632–2642, <https://doi.org/10.1145/3447548.3467182>, URL <https://doi.org/10.1145/3447548.3467182>

- Chen D, Lin Y, Li W, et al (2020) Measuring and relieving the over-smoothing problem for graph neural networks from the topological view. In: The Thirty-Fourth AAAI Conference on Artificial Intelligence, AAAI 2020, The Thirty-Second Innovative Applications of Artificial Intelligence Conference, IAAI 2020, The Tenth AAAI Symposium on Educational Advances in Artificial Intelligence, EAAI 2020, New York, NY, USA, February 7-12, 2020. AAAI Press, pp 3438–3445, URL <https://aaai.org/ojs/index.php/AAAI/article/view/5747>
- Chen T, Guestrin C (2016) Xgboost: A scalable tree boosting system. In: Proceedings of the 22nd ACM SIGKDD International Conference on Knowledge Discovery and Data Mining. Association for Computing Machinery, New York, NY, USA, KDD '16, p 785–794, <https://doi.org/10.1145/2939672.2939785>, URL <https://doi.org/10.1145/2939672.2939785>
- Deng S, Wang S, Rangwala H, et al (2020) Cola-gnn: Cross-location attention based graph neural networks for long-term ili prediction. In: Proceedings of the 29th ACM International Conference on Information & Knowledge Management. Association for Computing Machinery, New York, NY, USA, CIKM '20, p 245–254, <https://doi.org/10.1145/3340531.3411975>, URL <https://doi.org/10.1145/3340531.3411975>
- Derr T, Ma Y, Fan W, et al (2020) Epidemic graph convolutional network. In: Proceedings of the 13th International Conference on Web Search and Data Mining. Association for Computing Machinery, New York, NY, USA, WSDM '20, p 160–168, <https://doi.org/10.1145/3336191.3371807>, URL <https://doi.org/10.1145/3336191.3371807>
- DUBEY B, PATRA A, SRIVASTAVA PK, et al (2013) Modeling and analysis of an seir model with different types of nonlinear treatment rates. *Journal of Biological Systems* 21(03):1350,023. <https://doi.org/10.1142/S021833901350023X>, URL <https://doi.org/10.1142/S021833901350023X>, <https://arxiv.org/abs/https://doi.org/10.1142/S021833901350023X>
- Fang X, Huang J, Wang F, et al (2020) Constgat: Contextual spatial-temporal graph attention network for travel time estimation at baidu maps. In: Proceedings of the 26th ACM SIGKDD International Conference on Knowledge Discovery & Data Mining. Association for Computing Machinery, New York, NY, USA, KDD '20, p 2697–2705, <https://doi.org/10.1145/3394486.3403320>, URL <https://doi.org/10.1145/3394486.3403320>
- Feng X, Guo J, Qin B, et al (2017) Effective deep memory networks for distant supervised relation extraction. In: Proceedings of the 26th International Joint Conference on Artificial Intelligence. AAAI Press, IJCAI'17, p 4002–4008

- Fritz C, Dorigatti E, Rügamer D (2022) Combining graph neural networks and spatio-temporal disease models to improve the prediction of weekly covid-19 cases in germany. *Scientific Reports* 12. <https://doi.org/10.1038/s41598-022-07757-5>, URL <https://doi.org/10.1038/s41598-022-07757-5>
- Gao J, Sharma R, Qian C, et al (2021) Stan: spatio-temporal attention network for pandemic prediction using real-world evidence. *Journal of the American Medical Informatics Association* 28(4):733–743
- Guo K, Hu Y, Sun Y, et al (2021) Hierarchical graph convolution network for traffic forecasting. *Proceedings of the AAAI Conference on Artificial Intelligence* 35(1):151–159. <https://doi.org/10.1609/aaai.v35i1.16088>, URL <https://ojs.aaai.org/index.php/AAAI/article/view/16088>
- He S, Peng Y, Sun K (2020) Seir modeling of the covid-19 and its dynamics. *Nonlinear Dynamics* 101:1667–1680. <https://doi.org/10.1038/s41598-022-07757-5>, URL <https://doi.org/10.1038/s41598-022-07757-5>
- Jin D, Yu Z, Huo C, et al (2021a) Universal graph convolutional networks. In: Ranzato M, Beygelzimer A, Dauphin Y, et al (eds) *Advances in Neural Information Processing Systems*, vol 34. Curran Associates, Inc., pp 10,654–10,664, URL <https://proceedings.neurips.cc/paper/2021/file/5857d68cd9280bc98d079fa912fd6740-Paper.pdf>
- Jin X, Wang YX, Yan X (2021b) Inter-Series Attention Model for COVID-19 Forecasting, *SIAM*, pp 495–503. <https://doi.org/10.1137/1.9781611976700.56>, URL <https://epubs.siam.org/doi/abs/10.1137/1.9781611976700.56>, <https://epubs.siam.org/doi/pdf/10.1137/1.9781611976700.56>
- Kapoor A, Ben X, Liu L, et al (2020) Examining covid-19 forecasting using spatio-temporal graph neural networks. *arXiv preprint arXiv:200703113*
- Kara A (2021) Multi-step influenza outbreak forecasting using deep lstm network and genetic algorithm. *Expert Systems with Applications* 180:115,153. <https://doi.org/https://doi.org/10.1016/j.eswa.2021.115153>, URL <https://www.sciencedirect.com/science/article/pii/S0957417421005947>
- Kargas N, Qian C, Sidiropoulos ND, et al (2021) Stelar: Spatio-temporal tensor factorization with latent epidemiological regularization. *Proceedings of the AAAI Conference on Artificial Intelligence* 35(6):4830–4837. <https://doi.org/10.1609/aaai.v35i6.16615>, URL <https://ojs.aaai.org/index.php/AAAI/article/view/16615>
- Kim M, Kang J, Kim D, et al (2020) Hi-covidnet: Deep learning approach to predict inbound covid-19 patients and case study in south korea. In: *Proceedings of the 26th ACM SIGKDD International Conference on Knowledge Discovery & Data Mining*. Association for Computing Machinery, New

York, NY, USA, KDD '20, p 3466–3473, <https://doi.org/10.1145/3394486.3412864>, URL <https://doi.org/10.1145/3394486.3412864>

Kipf TN, Welling M (2017a) Semi-supervised classification with graph convolutional networks. In: 5th International Conference on Learning Representations, ICLR 2017, Toulon, France, April 24–26, 2017, Conference Track Proceedings. OpenReview.net, URL <https://openreview.net/forum?id=SJU4ayYgl>

Kipf TN, Welling M (2017b) Semi-supervised classification with graph convolutional networks. In: 5th International Conference on Learning Representations, ICLR 2017, Toulon, France, April 24–26, 2017, Conference Track Proceedings. OpenReview.net, URL <https://openreview.net/forum?id=SJU4ayYgl>

Lin H, Bai R, Jia W, et al (2020) Preserving dynamic attention for long-term spatial-temporal prediction. In: Proceedings of the 26th ACM SIGKDD International Conference on Knowledge Discovery & Data Mining. Association for Computing Machinery, New York, NY, USA, KDD '20, p 36–46, <https://doi.org/10.1145/3394486.3403046>, URL <https://doi.org/10.1145/3394486.3403046>

López L, Rodó X (2021) A modified seir model to predict the covid-19 outbreak in spain and italy: Simulating control scenarios and multi-scale epidemics. *Results in Physics* 21:103,746. <https://doi.org/https://doi.org/10.1016/j.rinp.2020.103746>, URL <https://www.sciencedirect.com/science/article/pii/S2211379720321604>

Maleki M, Mahmoudi MR, Wraith D, et al (2020) Time series modelling to forecast the confirmed and recovered cases of covid-19. *Travel Medicine and Infectious Disease* 37:101,742. <https://doi.org/https://doi.org/10.1016/j.tmaid.2020.101742>, URL <https://www.sciencedirect.com/science/article/pii/S1477893920302210>

Montero-Manso P, Athanasopoulos G, Hyndman RJ, et al (2020) Fforma: Feature-based forecast model averaging. *International Journal of Forecasting* 36(1):86–92. <https://doi.org/https://doi.org/10.1016/j.ijforecast.2019.02.011>, URL <https://www.sciencedirect.com/science/article/pii/S0169207019300895>, m4 Competition

Mussumeci E, Codeço Coelho F (2020) Large-scale multivariate forecasting models for dengue - lstm versus random forest regression. *Spatial and Spatio-temporal Epidemiology* 35:100,372. <https://doi.org/https://doi.org/10.1016/j.sste.2020.100372>, URL <https://www.sciencedirect.com/science/article/pii/S1877584520300502>

- Oreshkin BN, Carпов D, Chapados N, et al (2020) N-BEATS: neural basis expansion analysis for interpretable time series forecasting. In: 8th International Conference on Learning Representations, ICLR 2020, Addis Ababa, Ethiopia, April 26-30, 2020. OpenReview.net, URL <https://openreview.net/forum?id=r1ecqn4YwB>
- Panaggio MJ, Rainwater-Lovett K, Nicholas PJ, et al (2022) Gecko: A time-series model for covid-19 hospital admission forecasting. *Epidemics* 39:100,580. <https://doi.org/https://doi.org/10.1016/j.epidem.2022.100580>, URL <https://www.sciencedirect.com/science/article/pii/S1755436522000299>
- Panagopoulos G, Nikolentzos G, Vazirgiannis M (2021) Transfer graph neural networks for pandemic forecasting. *Proceedings of the AAAI Conference on Artificial Intelligence* 35(6):4838–4845. <https://doi.org/10.1609/aaai.v35i6.16616>, URL <https://ojs.aaai.org/index.php/AAAI/article/view/16616>
- Pei S, Shaman J (2020) Initial simulation of sars-cov2 spread and intervention effects in the continental us. *MedRxiv* pp 2020–03
- Qian Z, Alaa AM, van der Schaar M (2020) When and how to lift the lockdown? global covid-19 scenario analysis and policy assessment using compartmental gaussian processes. In: Larochelle H, Ranzato M, Hadsell R, et al (eds) *Advances in Neural Information Processing Systems*, vol 33. Curran Associates, Inc., pp 10,729–10,740, URL <https://proceedings.neurips.cc/paper/2020/file/79a3308b13cd31f096d8a4a34f96b66b-Paper.pdf>
- Ray EL, Wattanachit N, Niemi J, et al (2020) Ensemble forecasts of coronavirus disease 2019 (covid-19) in the us. *MedRxiv* pp 2020–08
- Rodríguez A, Muralidhar N, Adhikari B, et al (2021) Steering a historical disease forecasting model under a pandemic: Case of flu and covid-19. *Proceedings of the AAAI Conference on Artificial Intelligence* 35(6):4855–4863. <https://doi.org/10.1609/aaai.v35i6.16618>, URL <https://ojs.aaai.org/index.php/AAAI/article/view/16618>
- SHI X, Chen Z, Wang H, et al (2015) Convolutional lstm network: A machine learning approach for precipitation nowcasting. In: Cortes C, Lawrence N, Lee D, et al (eds) *Advances in Neural Information Processing Systems*, vol 28. Curran Associates, Inc., URL <https://proceedings.neurips.cc/paper/2015/file/07563a3fe3bbe7e3ba84431ad9d055af-Paper.pdf>
- Shuvo SB, Molokwu BC, Kobti Z (2020) Simulating the impact of hospital capacity and social isolation to minimize the propagation of infectious diseases. In: *Proceedings of the 26th ACM SIGKDD International Conference on Knowledge Discovery & Data Mining*. Association for Computing Machinery, New York, NY, USA, KDD '20, p 3451–3457, <https://doi.org/>

10.1145/3394486.3412859, URL <https://doi.org/10.1145/3394486.3412859>

Smyl S (2020) A hybrid method of exponential smoothing and recurrent neural networks for time series forecasting. *International Journal of Forecasting* 36(1):75–85. <https://doi.org/https://doi.org/10.1016/j.ijforecast.2019.03.017>, URL <https://www.sciencedirect.com/science/article/pii/S0169207019301153>, m4 Competition

Srivastava A, Xu T, Prasanna VK (2020) Fast and accurate forecasting of covid-19 deaths using the sikj model. *arXiv preprint arXiv:200705180*

To T, Zhang K, Maguire B, et al (2021) Correlation of ambient temperature and covid-19 incidence in canada. *Science of The Total Environment* 750:141,484. <https://doi.org/https://doi.org/10.1016/j.scitotenv.2020.141484>, URL <https://www.sciencedirect.com/science/article/pii/S0048969720350130>

Velickovic P, Cucurull G, Casanova A, et al (2018) Graph attention networks. In: 6th International Conference on Learning Representations, ICLR 2018, Vancouver, BC, Canada, April 30 - May 3, 2018, Conference Track Proceedings. OpenReview.net, URL <https://openreview.net/forum?id=rJXMpikCZ>

Wang L, Wang G, Gao L, et al (2020a) Spatiotemporal dynamics, now-casting and forecasting of covid-19 in the united states. *arXiv preprint arXiv:200414103*

Wang L, Adiga A, Chen J, et al (2022) Causalgnn: Causal-based graph neural networks for spatio-temporal epidemic forecasting. *Proceedings of the AAAI Conference on Artificial Intelligence* 36(11):12,191–12,199. <https://doi.org/10.1609/aaai.v36i11.21479>, URL <https://ojs.aaai.org/index.php/AAAI/article/view/21479>

Wang P, Zheng X, Ai G, et al (2020b) Time series prediction for the epidemic trends of covid-19 using the improved lstm deep learning method Case studies in russia, peru and iran. *Chaos, Solitons & Fractals* 140:110,214. <https://doi.org/https://doi.org/10.1016/j.chaos.2020.110214>, URL <https://www.sciencedirect.com/science/article/pii/S096007792030610X>

Wu Z, Pan S, Long G, et al (2020) Connecting the dots: Multivariate time series forecasting with graph neural networks. In: *Proceedings of the 26th ACM SIGKDD International Conference on Knowledge Discovery & Data Mining*. Association for Computing Machinery, New York, NY, USA, KDD '20, p 753–763, <https://doi.org/10.1145/3394486.3403118>, URL <https://doi.org/10.1145/3394486.3403118>

Xie F, Zhang Z, Li L, et al (2023) Epignn: Exploring spatial transmission with graph neural network for regional epidemic forecasting. In: Amini MR,

- Canu S, Fischer A, et al (eds) Machine Learning and Knowledge Discovery in Databases. Springer Nature Switzerland, Cham, pp 469–485
- Ye Y, Fan Y, Hou S, et al (2021) Community mitigation: A data-driven system for covid-19 risk assessment in a hierarchical manner. In: Proceedings of the 29th ACM International Conference on Information & Knowledge Management. Association for Computing Machinery, New York, NY, USA, CIKM '20, p 2909–2916, <https://doi.org/10.1145/3340531.3412753>, URL <https://doi.org/10.1145/3340531.3412753>
- Yu B, Yin H, Zhu Z (2018) Spatio-temporal graph convolutional networks: A deep learning framework for traffic forecasting. In: Proceedings of the 27th International Joint Conference on Artificial Intelligence. AAAI Press, IJCAI'18, p 3634–3640
- Zhao L, Song Y, Zhang C, et al (2020) T-gcn: A temporal graph convolutional network for traffic prediction. IEEE Transactions on Intelligent Transportation Systems 21(9):3848–3858. <https://doi.org/10.1109/TITS.2019.2935152>
- Zheng S, Gao Z, Cao W, et al (2021) Hierst: A unified hierarchical spatial-temporal framework for covid-19 trend forecasting. In: Proceedings of the 30th ACM International Conference on Information & Knowledge Management. Association for Computing Machinery, New York, NY, USA, CIKM '21, p 4383–4392, <https://doi.org/10.1145/3459637.3481927>, URL <https://doi.org/10.1145/3459637.3481927>